PCCP

Accepted Manuscript

ROYAL SOCIETY OF CHEMISTRY

www.rsc.org/pccp

Direct Electron Transfer of *Phanerochaete chrysosporium* Cellobiose Dehydrogenase at Platinum and Palladium Nanoparticle Decorated Carbon Nanotube Modified Electrodes

Somayyeh Bozorgzadeh[*, 1,2], Hassan Hamidi[1,2], Roberto Ortiz[1], Roland Ludwig[3] and Lo Gorton[*, 1]

[1]Department of Analytical Chemistry/Biochemistry and Structural Biology, Lund University, SE-22100 Lund, Sweden.

[2]Department of Chemistry, Zanjan Branch, Islamic Azad University, P O Box 49195-467, Zanjan, Iran.

[3] Vienna Institute of Biotechnology, Department of Food Sciences and Technology, BOKU-University of Natural Resources and Life Sciences, Vienna, Muthgasse 18, A-1190 Vienna, Austria

Abstract

In the present work, platinum and palladium nanoparticles (PtNPs and PdNPs) were decorated on the surface of multi-walled carbon nanotubes (MWCNTs) by a simple thermal decomposition method. The prepared nano hybrids, PtNPs-MWCNTs and PdNPs-MWCNTs, were cast on the surface of spectrographic graphite electrodes and then *Phanerochaete chrysosporium* cellobiose dehydrogenase (*Pc*CDH) was adsorbed

[*]Corresponding authors.
E-mail: somayehbozorgzadeh@gmail.com
Lo.Gorton@biochemistry.lu.se

on the modified layer. Direct electron transfer between *Pc*CDH and the nanostructured modified electrodes was studied using flow injection amperometry and cyclic voltammetry. The maximum current responses (I_{max}) and the apparent Michaelis-Menten constants (K_M^{app}) for the different *Pc*CDH modified electrodes were calculated by fitting the data to the Michaels-Menten equation and compared. The sensitivity towards lactose was 3.07 and 3.28 μA mM^{-1} at the *Pc*CDH/PtNPs-MWCNTs/SPGE and *Pc*CDH/PdNPs-MWCNTs/SPGE electrodes, respectively, which were higher than those measured at the *Pc*CDH/MWCNTs/SPGE (2.60 μA mM^{-1}) and *Pc*CDH/SPGE (0.92 μA mM^{-1}). The modified electrodes were additionally tested as a bioanode for biofuel cell applications.

Keywords: Cellobiose dehydrogenase, Direct electron transfer, Palladium nanoparticles, Platinum nanoparticles, Multi-walled carbon nanotubes, Lactose.

1. Introduction

Cellobiose dehydrogenase (CDH, EC 1.1.99.18) is an extracellular monomeric redox enzyme produced by both basidiomycetes (class I CDH) and ascomycetes (class II CDH). They all consist of a catalytically active, flavin adenine dinucleotide (FAD) containing dehydrogenase domain (DH_{CDH}), which is connected via a flexible linker region to a haem *b* containing cytochrome domain (CYT_{CDH}) [1, 2]. In biocatalysis the DH_{CDH} serves as the catalytic site, where the substrate is oxidised. The reduced FAD can be reoxidised through a sequential transfer of electrons to the CYT_{CDH}, which sequentially donates the electrons directly to the electrode acting like a one electron acceptor [1, 3]. The natural substrates for CDH are cellobiose and other cellodextrins that emanate from breakdown of wood and the natural electron acceptor for reduced CDH are the recently found copper-dependent lytic polysaccharide monooxygenas [4]. However, lactose, which is structurally similar to cellobiose is also a substrate for all CDHs, and several different class I CDHs have been studied for making lactose biosensors [5-10].

One of the main challenging tasks in the development of amperometric biosensors and enzymatic fuel cell devices is to obtain an efficient electrical communication of redox enzymes with electrodes surfaces resulting in high current outputs at low substrate concentrations, thus leading to sensitive sensors and enabling their miniaturization for invasive or implantable applications. Direct electron transfer (DET) between redox enzymes and electrodes has many advantages over indirect electrical shuttling by a mediator, mediated electron transfer (MET). DET avoids the use of mediator molecules and reduces potential interferences and side reactions. However, DET on different kinds of electrodes, such as gold and various carbon materials has been obtained only for a restricted number of redox proteins and enzymes due to large

distances between the prosthetic group in the active site of the enzyme and the electrode [11-20]. It is well-known that DET either requires a close proximity of the active site of the redox enzymes to the protein surface or needs a connection with the protein surface by a built in electron transfer pathway constructed by a chain of redox active cofactors or by an electric wire [21] [22]. Due to the difficulty for enzymes to attain effective direct communication, different kinds of strategies including modifications of electrodes surface [7, 22-27], biochemical engineering of the enzymes [28, 29] and cascade reactions [30] have been already innovated to either enhance the effective surface area and/or to increase the rate of DET by suitable orientations or attraction of the CDH molecule on the surface [3].

Nanostructured electrodes represent new classes of electrodes that can increase the output currents from electron transfer of enzyme based biosensors and enzymatic fuel cells (EFCs). Nanostructured electrodes in comparison with their bulk counterparts provide higher current densities by functioning as nanoscaled electrical wires, which facilitate the contact of the active sites of redox enzymes by providing a large surface area for protein binding [31-33]. Single-walled carbon nanotubes (SWCNTs) and multi-walled carbon nanotubes (MWCNTs) have attracted enormous interest from a broad range of specialists [34-37]. CNTs have also been used as a support and/or a skeleton for the formation of linear metal and metal oxide nanoparticle assemblies due to their large chemically active surface and stability. These nanohybrid materials, often referred to as “decorated carbon nanotubes” are a new class of hybrid materials with the integrated properties of two components and show promising applications in many research areas [38]. In recent years, it has also been shown that CDH based biosensors and EFCs also have better DET performance by incorporation of nanomaterials such as SWCNTs [7, 22, 25-27], MWCNTs [39], carbon nanoparticles (CNPs) [28] and gold NPs [23,

[40]. Therefore, we thought that the integration of CDH with nanohybrid systems consisting of metal nanoparticles and CNTs could combine the catalytic functions of the biomolecules with the unique electronic and catalytic properties of these nanomaterials and offer new opportunities for the development of new third-generation biosensors (based on DET) and EFCs with high performance.

Here we report on DET of a class I CDH from the basidiomycete *Phanerochaete chrysosporium* (*Pc*CDH) investigated on graphite electrodes modified with MWCNTs decorated with PtNPs and PdNPs. *Phanerochaete chrysosporium* is the most well studied CDH enzyme [23, 41, 42], and the crystal structures of the individual domains are available [4]. In addition, Class-I CDHs from basidiomycota show strong selectivity for only cellodextrins and lactose, which has made such CDHs possible candidates for making third-generation biosensor for lactose [1, 6, 43]. The prepared electrodes showed significant and efficient DET yielding high current densities for lactose as substrate. The rates of DET of *Pc*CDH measured as currents at the different modified electrodes were compared by using flow injection amperometry and cyclic voltammetry. The kinetic parameters and applicability as a bioanode of the different *Pc*CDH modified electrodes were evaluated for lactose under optimized conditions.

2- Experimental

2.1. Reagents and chemicals

All chemicals were of analytical reagent grade and used as supplied without further purifications except for the carbon nanotubes. Platinum (II) acetylacetonate (99.99% trace metals basis) was purchased from Sigma (St. Louis, MO, USA). Palladium (II) acetate (47% Pd) was obtained from Merck (Darmstadt, Germany). Multi-walled carbon nanotubes (MWCNTs, 95% purity, OD = 10–30 nm, ID = 5–10 nm and length = 0.5–500 μm) were purchased from Aldrich (Steinheim, Germany). Cytochrome *c*

(cyt *c*) from bovine heart and β-lactose were obtained from Sigma-Aldrich GmbH (Sigma-Aldrich Chemicals, Steinheim, Germany). All solutions were prepared with water (18 MΩ cm) purified with a PURELAB UHQ II system from ELGA Labwater (High Wycombe, UK).

2.2. Preparation of metal NP modified MWCNTs

PtNPs and PdNPs decorated MWCNTs were prepared according to a method reported previously [38] with slight modifications [44]. In brief, the treatment of MWCNTs was conducted by refluxing with 70% HNO_3 for 16 h, followed by filtering and thorough washing of the material with deionized water until pH 7.0 and then drying in a vacuum oven. The pretreated MWCNTs (8 mmol carbon equivalent) were dry mixed with platinum (II) acetylacetonate (0.08 mmol) powder using a mortar and pestle for about 30 min under ambient conditions to prepare PtNPs decorated MWCNTs with 1 mol% Pt loading. The solid, homogenous mixture of platinum (II) acetylacetonate and MWCNTs was then transferred to a glass vial and heated under nitrogen atmosphere in an oven to 450 ºC for 1 h and held isothermally for 3 h. The product was then collected as the PtNPs-MWCNTs. The PdNPs decorated MWCNTs were prepared through a similar procedure. In these experiments, palladium (II) acetate was manually mixed with MWCNTs and heated to the decomposition temperature of the salt at the given experimental conditions (ramped to 300 ºC for 1 h and held for 3 h).

2.3. Enzyme preparation

Cellobiose dehydrogenase from *Pc*CDH was obtained and purified as previously described [45]. The cyt *c* assay was performed to determine the homogeneous activity of the enzyme used by following the reduction of 20 µM cyt *c* (ε_{550} = 19.6 mM^{-1} cm^{-1}) in 80 mM sodium acetate buffer, pH 4.5, containing 30 mM lactose at 30 °C. One unit of

enzymatic activity is defined as the amount of enzyme that oxidizes 1 µmol of lactose per min under the assay conditions [46]. The activity of the used *Pc*CDH preparation was 17.9 U mL^{-1}.

2.4. Apparatus

A three-electrode flow-through amperometric wall-jet cell was used [47] and contained the working electrode (modified graphite electrodes), a reference electrode ($Ag|AgCl|KCl_{0.1M}$, +0.288 V versus SHE) and a counter electrode made of a platinum wire connected to a potentiostat (Zäta Elektronik, Höör, Sweden). The enzyme modified electrode was press fitted into a Teflon holder and inserted into the wall-jet cell and kept at a constant distance (ca. 1 mm) from the inlet nozzle. A 100 mM sodium acetate buffer (pH 4.5) was used as the carrier and propelled by a peristaltic pump (Gilson, Villier-le-Bel, France) at a flow rate of 0.5 mL min^{-1}. The potential range has been chosen to be between +0.14 and +0.79 V versus SHE in steps of 50 mV. Sodium acetate buffer solutions (100 mM) from pH 3.5 to pH 6.5 were used to investigate the pH dependency. 50 µL of different lactose solutions with different concentrations in the same sodium acetate buffer were injected into the carrier stream via a six-port injection valve (Rheodyne, Cotati, CA, USA). The electric current responses were recorded on a strip chart recorder (Kipp & Zonen, Delft, The Netherlands). Before performing any substrate injection into the flow system, the carrier buffer solution was continuously pumped until a stable background current was obtained.

Cyclic voltammetry was performed using an Autolab PGSTAT 30 from Metrohm (Utrecht, The Netherlands). As working electrode the modified graphite electrodes, a $Ag|AgCl|KCl_{sat}$ (+197 mV versus SHE) as reference electrode and a platinum foil as the auxiliary electrode was used. All CV studies were performed in a 100 mM sodium

acetate buffer solution at pH 4.5. Prior to CV experiments, the solutions were routinely deaerated by purging with high purity nitrogen gas for at least 20 min.

In bioanode performance studies, the Autolab PGSTAT 30 was used in potentiostatic mode. Polarization curves were recorded using linear sweep voltammetry (LSV) at a scan rate of 0.1 mV s^{-1} by connecting the bioanode (CDH-modified electrode) as the working electrode and the cathode (Pt black modified) as a combined reference and counter electrode. The measurements were done in a one-compartment 5 mL electrochemical cell containing 5 ml of 100 mM sodium acetate buffer (pH 4.5) and 5 mM lactose. All measurements were performed under air-saturated and quiescent conditions at room temperature.

Transmission electron microscopy (TEM) measurements were performed using a Philips CM 120 cryo-TEM instrument at 120 kV (Eindhoven, The Netherlands).

2.5. Fabrication of modified graphite electrodes

Rods of spectrographic graphite (SPGE, Alfa Aesar GmbH, Karlsruhe, Germany, AGKSP grade, Ø 3.05 mm) were used as working electrodes. The surface of the SPGE was prepared by polishing with fine emery paper (Tufback Durite, P1500), then thoroughly rinsed with Milli-Q water, and finally allowed to dry. One milligram of metal NPs-MWCNTs was dispersed in 1 mL of dimethylformamide (DMF) with ultrasonic agitation for 4 h to achieve a well-dispersed suspension. Then, 8 µL of the prepared metal NPs-MWCNTs suspensions (PtNPs-MWCNTs and PdNPs-MWCNTs) were cast on the surface of the SPGE and let to dry at room temperature to prepare SPGE modified with metal NPs decorated MWCNTs (PdNPs-MWCNTs/SPGE and PtNPs-MWCNTs/SPGE). Then, 3 µL of a *Pc*CDH solution with a volumetric activity of 17.9 U mL^{-1} was added on the surface of the NPs-MWCNTs/SPGE and allowed to dry in air at room-temperature and stored overnight

at 4 °C. Before each measurement, the electrodes were thoroughly rinsed with 100 mM sodium acetate buffer solution, pH 4.5 to remove weakly adsorbed enzyme molecules. For comparison, electrodes with no MWCNTs (*Pc*CDH/SPGE) and with MWCNTs without metal NPs (*Pc*CDH/MWCNTs/SPGE) were prepared using the same procedure described above.

3. Results and discussion

Our previous studies revealed that Au [48], Pd [49] and ZnO [50] NPs decorated MWCNTs nanohybrids had significant enhancing and fascinating effects on the electrochemical behavior of luminol and electrochemiluminescence performance of glucose and lactose biosensors. Hence, it was meaningful to investigate the synergetic enhancement effect of PtNPs and PdNPs and MWCNTs on the DET properties of CDHs [1, 3] and its possible application for the fabrication of a biosensors and EFC anodes.

3.1. Characterization of metal nanoparticle decorated carbon nanotubes

Figure 1 presents TEM images of (a) MWCNTs, (b) PtNPs-MWCNTs and (c) PdNPs-MWCNTs revealing the morphology of the MWCNTs after deposition of PtNPs and PdNPs. As can be observed in Figs. 1a and 1b, the sidewalls of the MWCNTs are covered with uniform sized PtNPs and PdNPs. The size distribution histograms presented on Figs. 1d and 1e for PtNPs-MWCNTs and PdNPs-MWCNTs, constructed from TEM images, give a mean value of 2.0 ± 0.3 and 3.7 ± 0.6 nm for the PtNPs and PdNPs, respectively.

Electrochemical characterization of the PtNPs-MWCNTs and PdNPs-MWCNTs on the surface of SPGEs was also performed by CV in 0.5 M H_2SO_4 solution at a scan rate of 50 mV s^{-1} (Supplementary information Fig. S1). The recorded CVs showed two main characteristic waves with one oxidation peak at 0.89 V and 1.07 V versus

SHE in the anodic scan associated with oxygen adsorption and one reduction peak at 0.69 V and 0.62 V versus SHE in the cathodic scan corresponding to oxygen striping at PtNPs-MWCNTs/SPGE and PdNPs-MWCNTs/SPGE, respectively. The anodic peaks at 0.1, 0.3 and 0.4 V versus SHE were attributed to the adsorption of hydrogen atoms at the PtNPs-MWCNTs/SPGE and PdNPs-MWCNTs/SPGE, respectively, as previously reported [44, 51]. The obtained results clearly proved that the PtNPs and PdNPs can be directly attached onto the surface of the MWCNTs by thermal decomposition of the acetate salts of the corresponding metal ions and without using any solvent, capping and reducing agent.

3.2. Flow injection amperometric measurements at the modified graphite electrodes

In order to investigate how the nanohybrid materials affect the electrocatalytical currents of the CDH-modified electrodes, the dependence of the bioelectrocatalytic oxidation of lactose on the amperometric responses of *Pc*CDH at PtNPs-MWCNTs/SPGE, PdNPs-MWCNTs/SPGE, MWCNTs/SPGE and SPGE modified electrodes was compared using flow injection amperometry. For basic investigations and characterization of CDH modified electrodes, lactose is the best substrate. It has a similar turn-over rate as cellobiose, but it does not show any substrate inhibition as cellobiose does [2].

The influence of pH on the current response of *Pc*CDH at the different modified SPGE surfaces towards lactose (1 mM) as substrate was investigated from 3.5 to 6.5 (Fig. 2a). As can be seen in Fig. 2a the current response increases from pH 3.5 to 4.5 and then decreases continuously until pH 6.5. These results are consistent with previous reports for the same CDH adsorbed onto SPGE and other electrode materials [6, 23, 52, 53]. As already reported the catalytic current based on DET on *Pc*CDH modified electrodes shows a strong dependence on pH attributed to the interaction between the

facing amino acids on the DH_{CDH} and the CYT_{CDH} [1, 2], which in turn determines the rate of the IET from the DH_{CDH} to the CYT_{CDH} and thus the catalytic current.

Figure 2b illustrates the effect of applied potential on the DET current response at the different modified electrodes. For this investigation, the applied potential was changed between +0.14 to +0.79 V versus SHE in steps of 50 mV and the current response was measured for each of the applied potentials by injecting 1 mM lactose (50 µL). Larger current responses for NPs modified electrodes were observed. (2.2, 3.5 and 4.2 fold) This can be explained by an increased effective surface area created by the MWCNTs on the surface of electrodes. However, when potentials higher than around 0.50 V versus SHE were applied, the current response of the different electrodes decreased significantly, probably due to the irreversible denaturation of the enzyme, which was previously reported for *Pc*CDH [54], *Sclerotium rolfsii* CDH [55], *Myriococcum thermophilum* CDH [56] and *Neurospora crassa* CDH [57].

The current responses of the different modified electrodes were recorded by injection of different concentrations of lactose in the flow-injection system using sodium acetate buffer as carrier buffer at pH 4.5 and at an applied potential of +0.49 V versus SHE. Figure 3 presents the current versus [lactose] plots of the different modified electrodes. The curves are fitted using the Michaelis-Menten equation. The electrodes modified with each of the different variants of MWCNTs showed significantly higher current responses than that registered for the *Pc*CDH/SPGE modified electrodes. The highest current densities were observed for the *Pc*CDH/PdNPs-MWCNTs/SPGE (53.8 µA cm^{-2}) and then for the *Pc*CDH/PtNPs-MWCNTs/SPGE (30.8 µA cm^{-2}), which is high compared with the *Pc*CDH/MWCNTs/SPGE (16.3 µA cm^{-2}) and at the *Pc*CDH/SPGE (8.2 µA cm^{-2}). The kinetic parameters; I_{max} (measured as maximum current response), K_M^{app} (apparent Michaelis–Menten constant) and I_{max}/K_M^{app} for the

all modified electrodes were calculated by fitting the data to the Michaelis-Menten equation, and shown in Table 1. From the obtained results it can be concluded that the modification of the SPGE with nanomaterials increased the sensitivity, and had almost no effect on the mass-transfer. Taking into consideration that the Michaelis–Menten constants remained virtually constant, one can conclude that the responses and sensitivities were just originated from the electrocatalytic activity, the electrical conductive network and the more effective surface area of the electrodes modified with nanomaterials.

Figure 4 presents successive injections of 1 mM lactose into the flow system for 10 h for *Pc*CDH/PtNPs-MWCNTs/SPGE and *Pc*CDH/PdNPs-MWCNTs/SPGE. The proposed electrodes kept approximately 85 and 75% of their initial response after 10 h of successive determinations, respectively, which must be regarded as excellent operational stability.

The high catalytic activity of *Pc*CDH/PdNPs-MWCNTs/SPGE toward lactose might be interesting for applications in context with the production of lactose free milk and in lactose measurements in other solutions in the dairy industry [9] or extending to the use of other types of CDH especially glucose mutants of CDH for biosensing and EFC applications [58].

3.3. Cyclic voltammetry of PcCDH at PtNPs-MWCNTs and PdNPs-MWCNTs modified graphite electrodes

The electrocatalytic properties of different nanomaterials on the DET properties of *Pc*CDH were investigated with CV in the potential range between -0.1 and 0.6 V versus SHE at a scan rate of 2 mV s^{-1} and the CVs were recorded and compared in the absence and presence of 5 mM lactose. The K_M^{app} value of *Pc*CDH for lactose was determined from flow measurements and found to be 0.65, 0.46, 0.73 and 1.2 mM at

*Pc*CDH/SPGE, *Pc*CDH/MWCNTs/SPGE *Pc*CDH/PtNPs-MWCNTs/SPGE and *Pc*CDH/PdNPs-MWCNTs/SPGE, the lactose concentration used for all further experiments (5 mM) is therefore 7.7, 10.9, 6.8 and 4.2-fold the K_M^{app} value of the enzyme mentioned prepared electrode surface and ensures a high catalytic substrate turnover (~80% of I_{max}). It is, on the other side, sufficiently low to avoid a significant background current by nonspecific oxidation as reported for a SWCNT modified electrode and a 100 mM lactose concentration [7, 22, 25-27]. Figure 5 shows CVs of *Pc*CDH on the surface of different graphite electrodes either (Fig. 5a) unmodified, (Fig. 5b) unmodified or (Figs. 5c and 5d) modified MWCNTs in the absence (solid line) and presence (dashed line) of 5 mM lactose in 100 mM sodium acetate buffer, pH 4.5. No visible peaks for the DET reaction of CYT_{CDH} were observed in the absence of substrate at the $E^{\circ\prime}$ of the CYT_{CDH} [1]. The results of *Pc*CDH on bare SPGE were not surprising, DET of CYTCDH in the absence of substrate has only been observed in this material for deglycosylated *Pc*CDH and deglycosylated *Ceriporiopsis subvermispora* CDH (*Cs*CDH) [28]. On the other hand, for CNT modified electrodes DET from CYT_{CDH} in the absence of substrate has been observed for *Phanerochaete sordida* CDH (*Ps*CDH), [22, 26, 27] and *Corynascus thermophilus* (*Ct*CDH) [58]. The reason for no visible waves for *Pc*CDH under non-turn over conditions might be the high capacitance currents obtained for the modified electrodes. However, the charging current densities obviously have been increased by the modification of SPGE with nanomaterials. It can be clearly seen that the order of increase in charging current is MWCNTs < PdNPs-MWCNTs < PtNPs-MWCNTS due to the significant increase in double layer capacitance of modified electrodes, respectively (Supplementary information Fig. S2). Since the double layer capacitance is also proportional to the effective surface area, it can thus be concluded that by

introducing nanostructured materials on the electrode surface will result in a significant improvement in the effective surface area, which in turn will cause the enhancement in the double layer capacitance and finally in charging current densities of the modified electrodes. In the presence of 5 mM lactose, a clear current increase is observed starting at approximately 100 mV versus SHE for all the modified electrodes studied. The observed increase is attributed to the electrocatalytical oxidation of the substrate by CDH and the DET between the CYT_{CDH} and the electrode as previously reported [1, 3]. The electrocatalytic current densities show the same trend as the effective surface area of the electrodes (Fig. 5, solid CVs). The possible reasons for this improvement can be the combined effects of the efficient electrical network of PtNPs and PdNPs on the surface of the MWCNTs and the higher loading of the *Pc*CDH on the electrode surface.

3.4. Studies of the bioanode performance of different modified electrodes

As a model for a membraneless enzymatic fuel cell, the capabilities of the designed electrodes to function as a bioanode were investigated together with a Pt black electrode as cathode [7, 22-27] in a 5 mM lactose solution in sodium acetate buffer solution at pH 4.5. Since the area of the cathode was much larger than that of the anode, the current density of this cell was limited by the anode [26, 27]. After an equilibration time of 10 min, a polarization curve was measured with linear sweep voltammetry (LSV) at a low scan rate (v = 0.1 mVs^{-1}) connecting the anode as working, and the cathode as reference and counter electrode. Figure 6 shows the LSVs and the dependence of the cell voltage versus the power density of the designed bioanodes. The maximum power density was 17.52 µW cm^{-2} at a cell voltage of 417 mV for the *Pc*CDH/PdNPs-MWCNTs/SPGE. The maximum power densities for *Pc*CDH/PtNPs-MWCNTs/SPGE (2.20 µW cm^{-2} at 293 mV), the

*Pc*CDH/MWCNTs/SPGE (5.80 μW cm^{-2} at 387 mV) and *Pc*CDH/SPGE (2.42 μW cm^{-2} at 322 mV) were significantly lower. In addition, the OCV for all electrodes was measured and summarized in Table 2. The OCV of the *Pc*CDH/PdNPs-MWCNTs/SPGE was also higher (78 and 32 mV) than those of the other mentioned electrodes. Based on the obtained results from CV (Supplementary information Fig. S2) and LSV (Table 2) studies, it seems that the smaller size of the NPs in comparison with the size of the enzyme molecules is expected to result in an enhancement effect on the bioelectrocatalytic signal in addition to the increased effective surface area. This proves the proposition that was made already on NPs with a size comparable to or less than enzyme molecules by reducing the electron tunneling distance of the electron transfer pathway. In contrast, by employing NPs larger than the enzyme molecule, the only possible reason for the improvement of bioelectrocatalytic signals could be the inherent effect of area magnification [59, 60]. Moreover, the operating voltages, at which the maximum power density is obtained, an important parameter for practical applications, of the *Pc*CDH/MWCNTs/SPGE, 387 mV and *Pc*CDH/PdNPs-MWCNTs/SPGE, 417 mV were significantly improved compared to that of the *Pc*CDH/SPGE, 322 mV. However, the obtained LSV and output power profile for the PtNPs-MWCNTs modified electrode (Fig. 6 dashed-dotted line) is completely different from the other modified electrodes. This inconsistent behavior may be the result from the ability of PtNPs-MWCNTs toward oxygen reduction that could cause the lowest current density and power density. The electrical power produced by the *Pc*CDH modified SPGE anode/Pt black cathode enzymatic fuel cell originates from the two electrocatalytic processes occurring simultaneously on the electrodes, via bioelectrooxidation of lactose on the anode and electroreduction of O_2 on the cathode.

Another important aspect of the designed EFC is its mixed operational/long-term stability, which was investigated by multicycle LSVs at a low scan rate (0.1 $mV \cdot s^{-1}$) using the best performing modified electrode, i.e. *Pc*CDH/PdNPs-MWCNTs/SPGE (Fig. 7). The designed bioanode showed good stability, i.e., with only a 20% drop in power density after 6 h of continuous operation which was extended for 10 h.

By replacing the Pt cathode by a laccase or bilirubin oxidase modified cathode [61-64], the maximum voltage of the cell is expected to be further increased. On the other hand, the increased OCV, good stability and simple preparation of the proposed bioanode make it interesting to replace *Pc*CDH with other types of CDHs especially CDHs of class II, e.g., *Myriococcum thermophilum* CDH [65], *Neurospora crassa* CDH [57], and the mutant of *Corynascus thermophilus* CDH with an increased glucose turn over rate [58].

4. Conclusions

The electrocatalytic activities of different nanomaterials on the DET of a class I CDH, *Phanerochaete chrysosporium* CDH, were investigated when deposited on the surface of graphite electrodes. It is shown that platinum and palladium nanoparticles can be directly added on the surface of MWCNTs by a solvent and reducing agent free method. The use of these metal NPs onto MWCNTs promotes the immobilisation of *Pc*CDH and increases the bioelectrocatalytic current and the sensitivity for lactose through providing an efficient electrical connection, a much higher and more effective surface area and a higher enzyme loading. Interestingly, the maximum current density, power output, OCV of the *Pc*CDH/PdNPs-MWCNTs/SPGE modified graphite electrode toward lactose were increased by 6.55, 7.24-folds and 78 mV in comparison to that on the *Pc*CDH/SPGE, respectively. The remarkable sensitivity,

stability and power density recommend the *Pc*CDH/PdNPs-MWCNTs/SPGE as a promising bioelectrode for the construction and development of third-generation biosensors and enzymatic fuel cells.

5. Acknowledgements

The authors thank The Swedish Research Council (projects 2007-4124, 2009-3266, 2010-5031, and 2014-5908), The European Commission (FP7 project NMP4-SL-2009-229255) and The Nanometer Consortium at Lund University (nmC@Lund) for financial support.

6. References

1 R. Ludwig, W. Harreither, F. Tasca and L. Gorton, *ChemPhysChem*, 2010, **11**, 2674-2697.
2 M. Zamocky, R. Ludwig, C. Peterbauer, B. M. Hallberg, C. Divne, P. Nicholls and D. Haltrich, *Curr. Protein. Pept. Sci*, 2006, **7**, 255-280.
3 R. Ludwig, R. Ortiz, C. Schulz, W. Harreither, C. Sygmund and L. Gorton, *Anal. Bioanal. Chem.*, 2013, **405**, 3637-3658.
4 T. C. Tan, D. Kracher, R. Gandini, C. Sygmund, R. Kittl, D. Haltrich, B. M. Hallberg, R. Ludwig and C. Divne, *Nat. Commun.*, 2015, **6**, 7542.
5 G. Safina, R. Ludwig and L. Gorton, *Electrochim. Acta*, 2010, **55**, 7690-7695.
6 T. Larsson, A. Lindgren, T. Ruzgas, S. E. Lindquist and L. Gorton, *J. Electroanal. Chem.*, 2000, **482**, 1-10.
7 F. Tasca, M. N. Zafar, W. Harreither, G. Noell, R. Ludwig and L. Gorton, *Analyst*, 2011, **136**, 2033-2036.
8 L. Stoica, R. Ludwig, D. Haltrich and L. Gorton, *Anal. Chem.*, 2006, **78**, 393-398.
9 N. Glithero, C. Clark, L. Gorton, W. Schuhmann and N. Pasco, *Anal. Bioanal. Chem.*, 2013, **405**, 3791-3799.
10 F. Tasca, R. Ludwig, L. Gorton and R. Antiochia, *Sens. Actuat. B: Chem.*, 2013, **177**, 64-69.
11 Y. Liu, Y. Du and C. M. Li, *Electroanalysis*, 2013, **25**, 815-831.
12 A. L. Ghindilis, P. Atanasov and E. Wilkins, *Electroanalysis*, 1997, **9**, 661-674.
13 A. Christenson, N. Dimcheva, E. E. Ferapontova, L. Gorton, T. Ruzgas, L. Stoica, S. Shleev, A. I. Yaropolov, D. Haltrich and R. N. Thorneley, *Electroanalysis*, 2004, **16**, 1074-1092.
14 L. Gorton, A. Lindgren, T. Larsson, F. Munteanu, T. Ruzgas and I. Gazaryan, *Anal. Chim. Acta*, 1999, **400**, 91-108.

15 C. Léger and P. Bertrand, *Chem. Rev.*, 2008, **108**, 2379-2438.
16 Y. Wu and S. Hu, *Microchim. Acta*, 2007, **159**, 1-17.
17 E. E. Ferapontova, S. Shleev, T. Ruzgas, L. Stoica, A. Christenson, J. Tkac, A. I. Yaropolov and L. Gorton, in *Perspectives in Bioanalysis*, eds. E. Paleček, F.W. Scheller and J. Wang, Elsevier, 2005, vol. 1, pp. 517-598.
18 W. Zhang and G. Li, *Anal. Sci.*, 2004, **20**, 603-609.
19 U. Wollenberger, in *Biosensors and Modern Biospecific Analytical Techniques*, ed. L. Gorton, Elsevier, Amsterdam, 2005, pp. 65-130.
20 M. Falk, Z. Blum and S. Shleev, *Electrochim. Acta*, 2012, **82**, 191-202.
21 F. A. Armstrong, H. A. O. Hill and N. J. Walton, *Acc. Chem. Res.*, 1988, **21**, 407-413.
22 F. Tasca, W. Harreither, R. Ludwig, J. J. Gooding and L. Gorton, *Anal. Chem.*, 2011, **83**, 3042-3049.
23 H. Matsumura, R. Ortiz, R. Ludwig, K. Igarashi, M. Samejima and L. Gorton, *Langmuir*, 2012, **28**, 10925-10933.
24 S. A. Trashin, D. Haltrich, R. Ludwig, L. Gorton and A. A. Karyakin, *Bioelectrochemistry*, 2009, **76**, 87-92.
25 F. Tasca, L. Gorton, W. Harreither, D. Haltrich, R. Ludwig and G. Nöll, *Anal. Chem.*, 2009, **81**, 2791-2798.
26 F. Tasca, L. Gorton, W. Harreither, D. Haltrich, R. Ludwig and G. Nöll, *J. Phys. Chem. C*, 2008, **112**, 9956-9961.
27 F. Tasca, L. Gorton, W. Harreither, D. Haltrich, R. Ludwig and G. Nöll, *J. Phys. Chem. C*, 2008, **112**, 13668-13673.
28 R. Ortiz, H. Matsumura, F. Tasca, K. Zahma, M. Samejima, K. Igarashi, R. Ludwig and L. Gorton, *Anal. Chem.*, 2012, **84**, 10315-10323.
29 M. Shao, M. N. Zafar, C. Sygmund, D. A. Guschin, R. Ludwig, C. K. Peterbauer, W. Schuhmann and L. Gorton, *Biosens. Bioelectron.*, 2013, **40**, 308-314.
30 M. N. Zafar, M. Shao, R. Ludwig, D. Leech, W. Schuhmann and L. Gorton, *ECS Transact.*, 2013, **53**, 131-143.
31 M. Pumera, S. Sánchez, I. Ichinose and J. Tang, *Sens. Actuat. B: Chem.*, 2007, **123**, 1195-1205.
32 R. S. Luz, R. Iost and F. Crespilho, in *Nanobioelectrochemistry*, ed. F. N. Crespilho, Springer Berlin Heidelberg, 2013, ch. 2, pp. 27-48.
33 A. Walcarius, S. D. Minteer, J. Wang, Y. Lin and A. Merkoci, *J. Mater. Chem. B*, 2013, **1**, 4878-4908.
34 C. B. Jacobs, M. J. Peairs and B. J. Venton, *Anal. Chim. Acta*, 2010, **662**, 105-127.
35 J. Wang, *Electroanalysis*, 2005, **17**, 7-14.
36 H.-M. So, K. Won, Y. H. Kim, B.-K. Kim, B. H. Ryu, P. S. Na, H. Kim and J.-O. Lee, *J. Am. Chem. Soc.*, 2005, **127**, 11906-11907.
37 J. N. Wohlstadter, J. L. Wilbur, G. B. Sigal, H. A. Biebuyck, M. A. Billadeau, L. Dong, A. B. Fischer, S. R. Gudibande, S. H. Jameison, J. H. Kenten, J. Leginus, J. K. Leland, R. J. Massey and S. J. Wohlstadter, *Adv. Mater.*, 2003, **15**, 1184-1187.
38 Y. Lin, K. A. Watson, M. J. Fallbach, S. Ghose, J. G. Smith, D. M. Delozier, W. Cao, R. E. Crooks and J. W. Connell, *ACS Nano*, 2009, **3**, 871-884.
39 M. N. Zafar, G. Safina, R. Ludwig and L. Gorton, *Anal. Biochem.*, 2012, **425**, 36-42.
40 X. Wang, M. Falk, R. Ortiz, H. Matsumura, J. Bobacka, R. Ludwig, M. Bergelin, L. Gorton and S. Shleev, *Biosens. Bioelectron.*, 2012, **31**, 219-225.

41 B. Martin Hallberg, G. Henriksson, G. Pettersson and C. Divne, *J. Mol. Biol.*, 2002, **315**, 421-434.
42 B. M. Hallberg, T. Bergfors, K. Bäckbro, G. Pettersson, G. Henriksson and C. Divne, *Structure*, 2000, **8**, 79-88.
43 L. Stoica, T. Ruzgas, R. Ludwig, D. Haltrich and L. Gorton, *Langmuir*, 2006, **22**, 10801-10806.
44 B. Haghighi, H. Hamidi and S. Bozorgzadeh, *Anal. Bioanal. Chem.*, 2010, **398**, 1411-1416.
45 G. Henriksson, G. Pettersson, G. Johansson, A. Ruiz and E. Uzcategui, *Eur. J. Biochem.*, 1991, **196**, 101-106.
46 U. Baminger, S. S. Subramaniam, V. Renganathan and D. Haltrich, *Appl. Environ. Microbiol.*, 2001, **67**, 1766-1774.
47 R. Appelqvist, G. Marko-Varga, L. Gorton, A. Torstensson and G. Johansson, *Anal. Chim. Acta*, 1985, **169**, 237-247.
48 B. Haghighi, S. Bozorgzadeh and L. Gorton, *Sens. Actuat. B: Chem.*, 2011, **155**, 577-583.
49 B. Haghighi and S. Bozorgzadeh, *Anal. Chim. Acta*, 2011, **697**, 90-97.
50 B. Haghighi and S. Bozorgzadeh, *Talanta*, 2011, **85**, 2189-2193.
51 S. Guerin and G. S. Attard, *Electrochem. Commun.*, 2001, **3**, 544-548.
52 A. Lindgren, L. Gorton, T. Ruzgas, U. Baminger, D. Haltrich and M. Schulein, *J. Electroanal. Chem.*, 2001, **496**, 76-81.
53 A. Lindgren, T. Larsson, T. Ruzgas and L. Gorton, *J. Electroanal. Chem.*, 2000, **494**, 105-113.
54 A. Lindgren, T. Ruzgas, L. Gorton, L. Stoica and A. Ciucu, *Analyst*, 1999, **124**, 527-532.
55 L. Stoica, A. Lindgren-Sjölander, T. Ruzgas and L. Gorton, *Anal. Chem.*, 2004, **76**, 4690-4696.
56 W. Harreither, V. Coman, R. Ludwig, D. Haltrich and L. Gorton, *Electroanalysis*, 2007, **19**, 172-180.
57 G. Kovacs, R. Ortiz, V. Coman, W. Harreither, I. C. Popescu, R. Ludwig and L. Gorton, *Bioelectrochemistry*, 2012, **88**, 84-91.
58 R. Ortiz, R. Ludwig and L. Gorton, *ChemElectroChem*, 2014, **1**, 1948-1956.
59 D. Pankratov, R. Sundberg, D. B. Suyatin, J. Sotres, A. Barrantes, T. Ruzgas, I. Maximov, L. Montelius and S. Shleev, *RSC Adv.*, 2014, **4**, 38164.
60 K. Monsalve, M. Roger, C. Gutierrez-Sanchez, M. Ilbert, S. Nitsche, D. Byrne-Kodjabachian, V. Marchi and E. Lojou, *Bioelectrochemistry*, 2015, DOI: 10.1016/j.bioelechem.2015.04.010.
61 A. Heller, *Phys. Chem. Chem. Phys.*, 2004, **6**, 209-216.
62 V. Coman, C. Vaz-Dominguez, R. Ludwig, W. Harreither, D. Haltrich, A. L. De Lacey, T. Ruzgas, L. Gorton and S. Shleev, *Phys. Chem. Chem. Phys.*, 2008, **10**, 6093-6096.
63 V. Coman, R. Ludwig, W. Harreither, D. Haltrich, L. Gorton, T. Ruzgas and S. Shleev, *Fuel Cells*, 2010, **10**, 9-16.
64 M. Falk, V. Andoralov, Z. Blum, J. Sotres, D. B. Suyatin, T. Ruzgas, T. Arnebrant and S. Shleev, *Biosens. Bioelectron.*, 2012, **37**, 38-45.
65 M. Shao, M. N. Zafar, M. Falk, R. Ludwig, C. Sygmund, C. K. Peterbauer, D. A. Guschin, D. MacAodha, P. Ó Conghaile, D. Leech, M. D. Toscano, S. Shleev, W. Schuhmann and L. Gorton, *ChemPhysChem*, 2013, **14**, 2260-2269.

Legend to figures:

Fig. 1. TEM images of MWCNTs (a), PtNPs-MWCNTs (b) and PdNPs-MWCNTs (c) and histograms of PtNPs-MWCNTs (d) and PdNPs-MWCNTs (e).

Fig. 2. (a) pH profiles and (b) dependence of the current on the applied potential for (◆) *Pc*CDH, (■) *Pc*CDH/MWCNTs, (▲) *Pc*CDH/PtNPs-MWCNTs, and (○) *Pc*CDH/PdNPs-MWCNTs modified graphite electrodes. Conditions: 1 mM lactose; carrier buffer, 0.1 M sodium acetate buffer (pH 4.5); flow rate, 0.5 mL min^{-1}.

Fig. 3. Dependence of the amperometric FIA response towards lactose concentration at (◆) *Pc*CDH, (■) *Pc*CDH/MWCNTs, (▲) *Pc*CDH/PtNPs-MWCNTs, and (○) *Pc*CDH/PdNPs-MWCNTs modified graphite electrodes. Conditions: E_{app} versus SHE, + 0.49 V; carrier buffer, 0.1 M sodium acetate buffer (pH 4.5); flow rate, 0.5 mL min^{-1}.

Fig. 4. Variation of the amperometric FIA response with time for successive injection of 1 mM lactose at a (▲) *Pc*CDH/PtNPs-MWCNTs and (○) *Pc*CDH/PdNPs-MWCNTs modified graphite electrode. Conditions: E_{app} versus SHE, +0.49 V; carrier buffer, 0.1 M acetate buffer (pH 4.5); flow rate, 0.5 mL min^{-1}.

Fig. 5. CVs of a (a) *Pc*CDH, (b) *Pc*CDH/MWCNTs, (c) *Pc*CDH/PtNPs-MWCNTs and (d) *Pc*CDH/PdNPs-MWCNTs modified graphite electrodes in the absence (solid line) and presence (dashed line) of 5 mM lactose. Conditions: supporting electrolyte, 0.1 M sodium acetate buffer (pH 4.5); potential scan rate, 2 mV s^{-1}.

Fig. 6. (a) Typical LSV and (b) the dependence of the power density on the cell voltage for a membrane-less biofuel cell consisting of a *Pc*CDH (dotted line), *Pc*CDH/MWCNTs (dashed line) *Pc*CDH/PtNPs-MWCNTs (dashed-dotted line) and *Pc*CDH/PdNPs-MWCNTs (solid line) and modified graphite electrodes as a bioanode and a Pt black electrode as cathode in air-saturated quiescent solutions. Conditions:

fuel, 5 mM lactose; supporting electrolyte, 0.1 M sodium acetate buffer (pH 4.5); potential scan rate, 0.1 mV s^{-1}.

Fig. 7. Variation of the dependence of the power density on the cell voltage for a membrane-less biofuel cell consisting of *Pc*CDH/PdNPs-MWCNTs electrodes as a bioanode and a Pt black electrode as cathode in air-saturated quiescent solutions during 6 consecutive cycles. Conditions: fuel, 5 mM lactose; supporting electrolyte, 0.1 M sodium acetate buffer (pH 4.5); potential scan rate, 0.1 mV s^{-1}.

Table 1. Kinetic parameters for different *Pc*CDH modified graphite electrodes calculated from values shown in Fig. 3**.**

Table 2. A comparison of potentially DET-based BFCs. Calculated from Fig. 6.

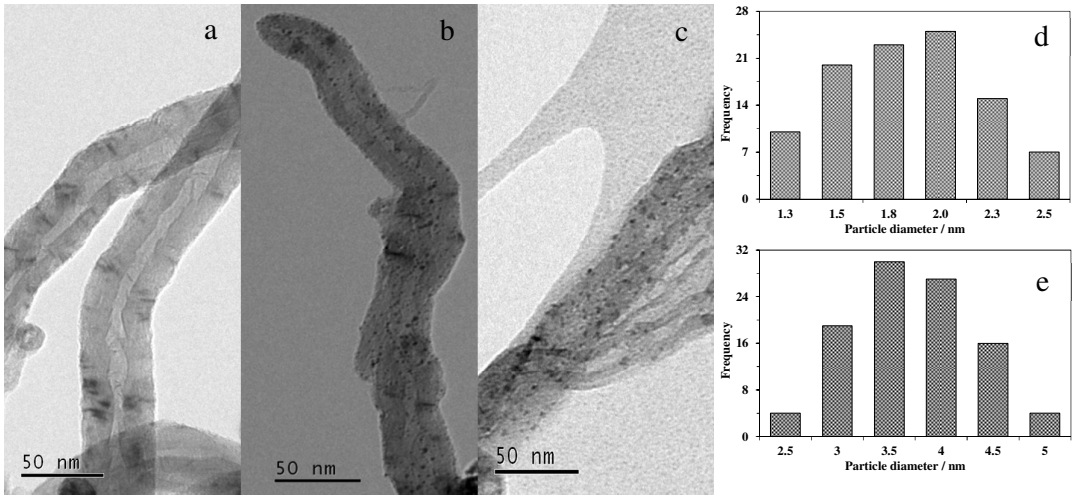

Fig.1

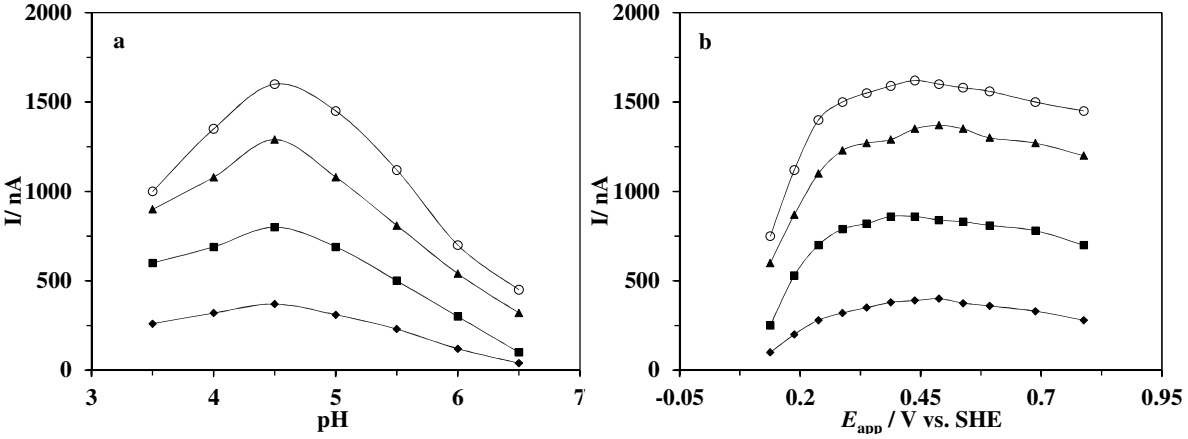

Fig. 2

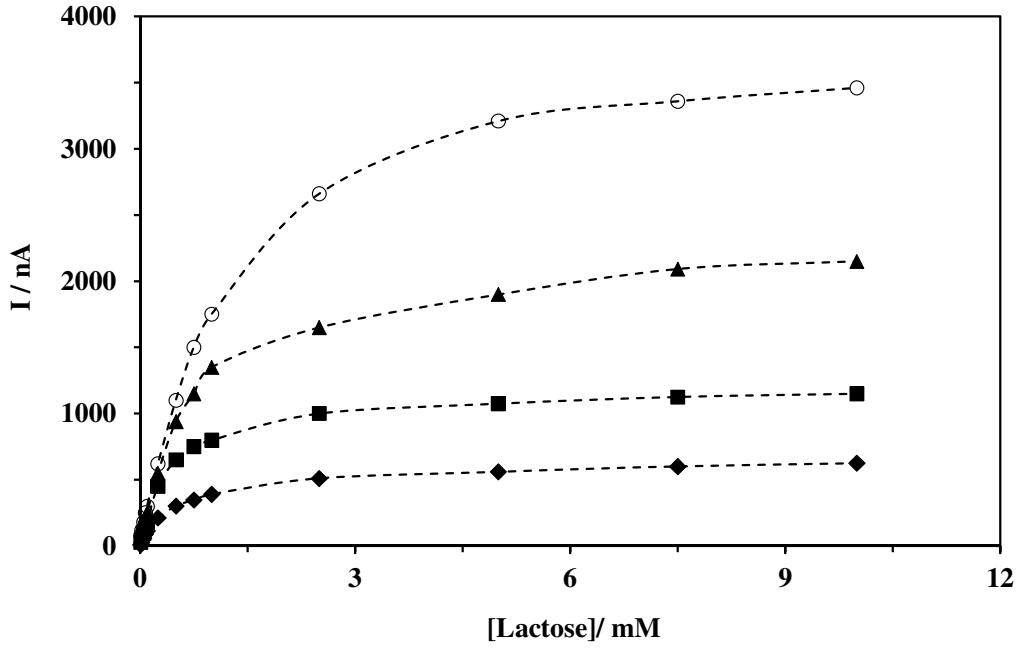

Fig.3

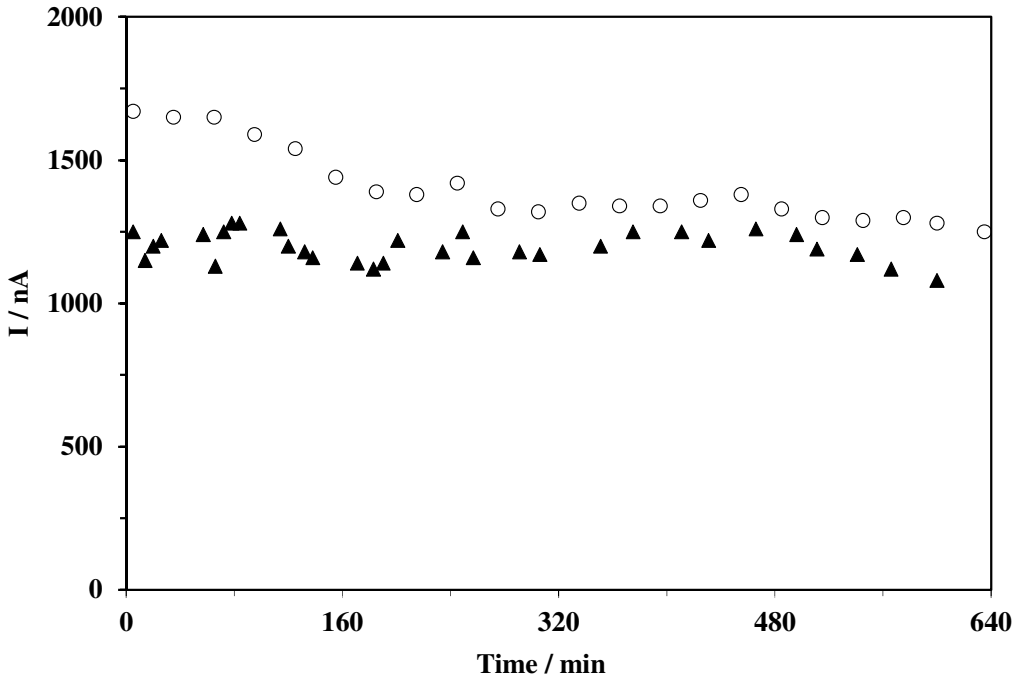

Fig.4

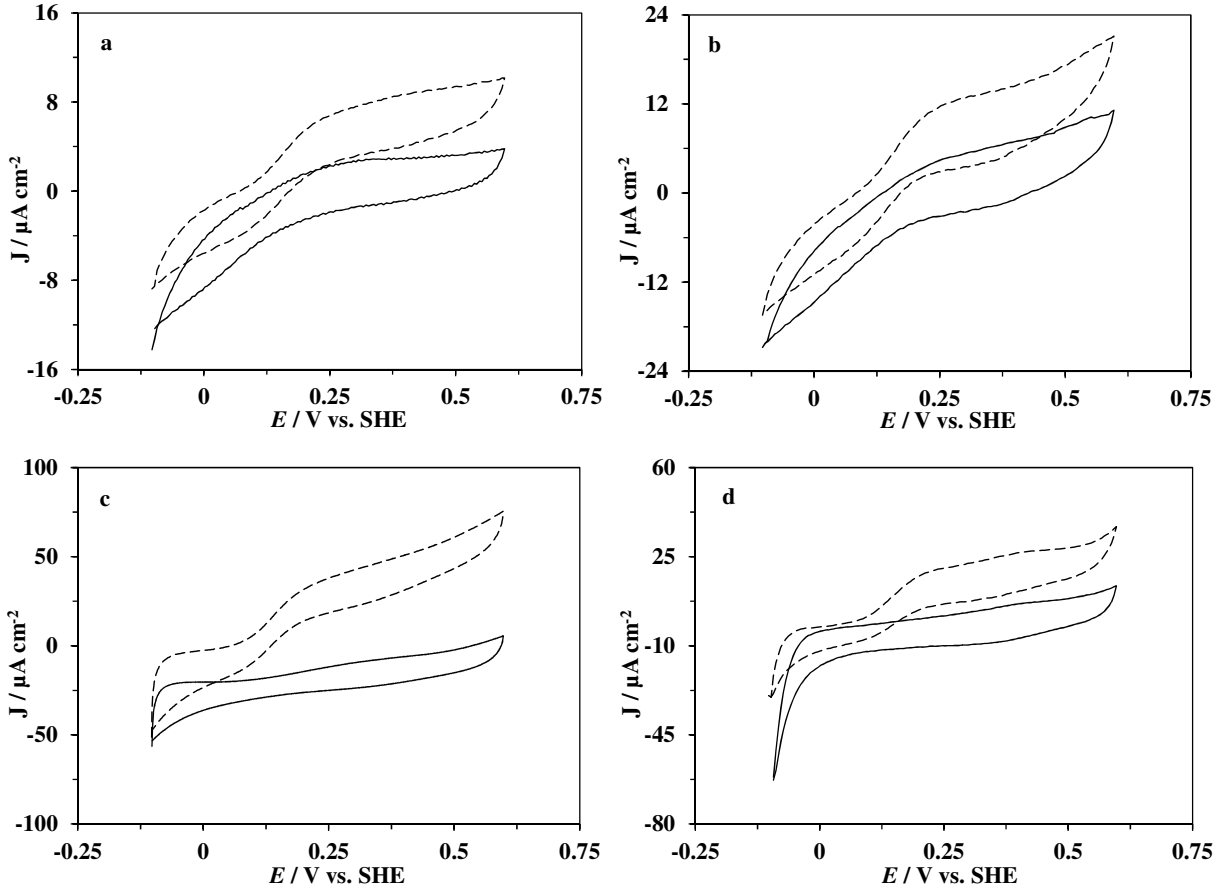

Fig. 5

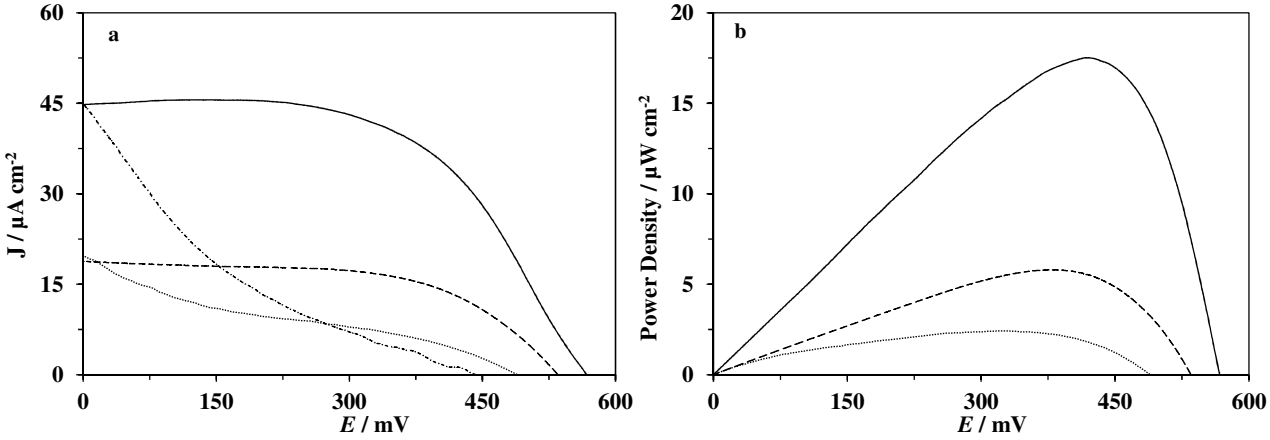

Fig.6

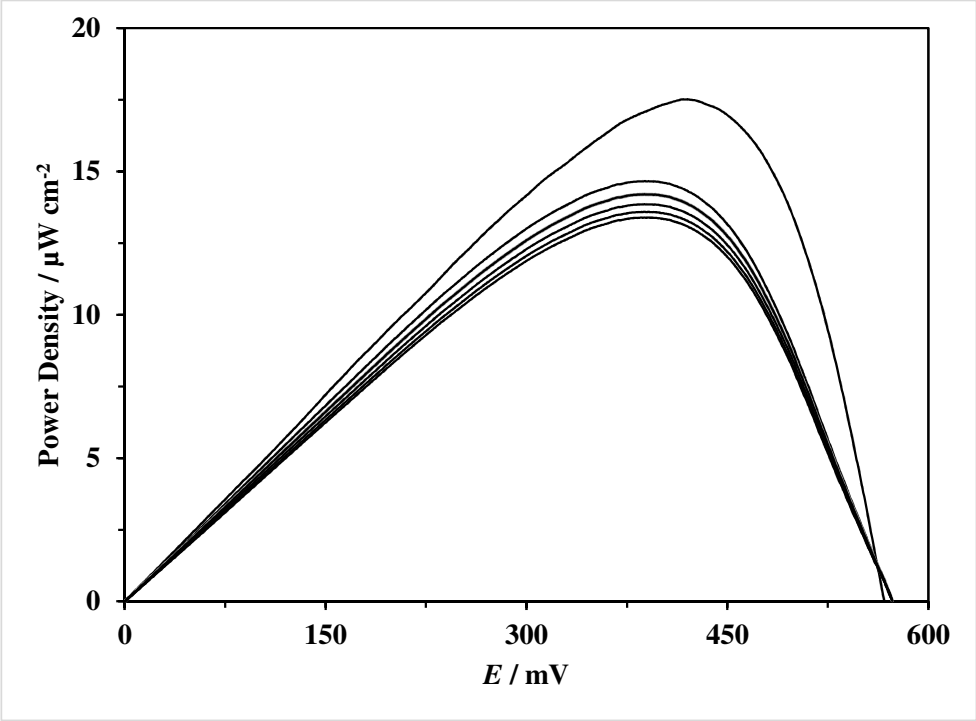

Fig.7

Table 1. Kinetic parameters for different *Pc*CDH modified graphite electrodes calculated from values shown in Fig. 3**.**

Modified electrodes	$\mathbf{I_{max}/\mu A}$	$\boldsymbol{K_M^{app}}$**/mM**	$\mathbf{(I_{max}/K_M^{app})/\mu A mM^{-1}}$
*Pc*CDH/SPGE	0.60 (± 0.01)	0.65 (± 0.06)	0.92
*Pc*CDH/MWCNTs/SPGE	1.19 (±0.01)	0.46 (±0.02)	2.60
*Pc*CDH/PtNPs-MWCNTs/SPGE	2.25 (±0.03)	0.73 (±0.04)	3.07
*Pc*CDH/PdNPs-MWCNTs/SPGE	3.93 (±0.04)	1.20 (±0.04)	3.28

Table 2. A comparison of potentially DET-based BFCs.

Modified electrodes	**OCV/mV**	**Power output/**μWcm^{-2}
*Pc*CDH/SPGE	489	2.42 at 322 mV
*Pc*CDH/MWCNTs/SPGE	535	5.80 at 387 mV
*Pc*CDH/PtNPs-MWCNTs/SPGE	442	2.20. at 293 mV
*Pc*CDH/PdNPs-MWCNTs/SPGE	567	17.52 at 417 mV